The EMBO Journal (2011) 30, 3416–3429 | © 2011 European Molecular Biology Organization | All Rights Reserved 0261-4189/11
www.embojournal.org

THE EMBO JOURNAL

Sunday Driver/JIP3 binds kinesin heavy chain directly and enhances its motility

Faneng Sun[1], Chuanmei Zhu[2], Ram Dixit[2] and Valeria Cavalli[1,*]

[1]Department of Anatomy and Neurobiology, Washington University in St Louis, School of Medicine, St Louis, MO, USA and [2]Department of Biology, Washington University in St Louis, St Louis, MO, USA

Neuronal development, function and repair critically depend on axonal transport of vesicles and protein complexes, which is mediated in part by the molecular motor kinesin-1. Adaptor proteins recruit kinesin-1 to vesicles via direct association with kinesin heavy chain (KHC), the force-generating component, or via the accessory light chain (KLC). Binding of adaptors to the motor is believed to engage the motor for microtubule-based transport. We report that the adaptor protein Sunday Driver (syd, also known as JIP3 or JSAP1) interacts directly with KHC, in addition to and independently of its known interaction with KLC. Using an *in vitro* motility assay, we show that syd activates KHC for transport and enhances its motility, increasing both KHC velocity and run length. syd binding to KHC is functional in neurons, as syd mutants that bind KHC but not KLC are transported to axons and dendrites similarly to wild-type syd. This transport does not rely on syd oligomerization with itself or other JIP family members. These results establish syd as a positive regulator of kinesin activity and motility.

The EMBO Journal (2011) **30,** 3416–3429. doi:10.1038/emboj.2011.229; Published online 12 July 2011
Subject Categories: membranes & transport; neuroscience
Keywords: axonal transport; JIP3; kinesin; motility; syd

Introduction

Neurons are extremely polarized cells with specialized domains including a long axon and multiple dendrites. Most proteins needed to function in axons and dendrites are synthesized in the cell body and transported to their final destination. This intracellular transport is essential for neuronal development, maintenance, and function. The kinesin family of motor proteins primarily drives the anterograde transport of cargoes towards distal areas of the neuron. Kinesin uses the energy of ATP hydrolysis to generate the motile force that moves cargo towards the plus-end of microtubules. The neuronal kinesin-1, known as conventional kinesin, drives the transport of a variety of molecules including protein complexes, vesicles, RNA granules, and cytoskeletal components (reviewed in Guzik and Goldstein, 2004; Goldstein *et al*, 2008 and Hirokawa *et al*, 2009).

Kinesin-1 conventionally refers to a tetramer of two heavy chains (KHC or KIF5), which harbour the motor domain, and two accessory light chains (KLC), which do not posses any motor activity (Verhey and Hammond, 2009). The association of cargoes to kinesin-1 is mediated by adaptor proteins that directly bind either KHC or KLC (Hirokawa *et al*, 2009). Over 20 adaptor proteins have now been identified. Adaptor proteins that interact with KHC directly to mediate the transport of diverse organelles and protein complexes include Milton (Glater *et al*, 2006), mRNP complex (Kanai *et al*, 2004), syntabulin (Su *et al*, 2004; Cai *et al*, 2005), SNAP25 (Diefenbach *et al*, 2002), DISC1 (Taya *et al*, 2007), GRIP1 (Setou *et al*, 2002), Fez1/unc76 (Gindhart *et al*, 2003; Blasius *et al*, 2007), RanPB2 (Cho *et al*, 2007), mNUDC (Yamada *et al*, 2010), and bicaudal D1/D2 (Grigoriev *et al*, 2007). Adaptor proteins also interact with KLC to mediate transport and include the JIP family of proteins (Bowman *et al*, 2000; Verhey *et al*, 2001; Kelkar *et al*, 2005; Nguyen *et al*, 2005), APP (Kamal *et al*, 2000), kiddins/ARMS (Bracale *et al*, 2007), alcadein (Araki *et al*, 2007), CRMP2 (Kimura *et al*, 2005), caytaxin (Aoyama *et al*, 2009), calsyntenin (Konecna *et al*, 2006), nesprins (Roux *et al*, 2009), and Hsc70 (Terada *et al*, 2010). The Fragile X mental retardation protein (FMRP) interacts with KLC to mediate the transport of mRNA granules in mouse neurons but does not require KLC in Drosophila S2 cells (Ling *et al*, 2004; Dictenberg *et al*, 2008). The growing number of identified KLC and KHC binding partners is thought to reflect the complexity of the molecular machinery controlling kinesin-1's cargo selectivity.

The binding of adaptors to kinesin-1 is also believed to promote activation of the motor for microtubule binding and motility. When not transporting cargo, kinesin-1 is thought to be inactive due to a folded conformation positioning the KHC tail domain near the enzymatically active motor domain, thereby preventing ATP hydrolysis (reviewed in Verhey and Hammond, 2009). The KHC tail has also been shown to contain an ATP-independent microtubule-binding domain, which was suggested to 'park' kinesin on microtubules when not transporting cargo (Dietrich *et al*, 2008; Seeger and Rice, 2010; Watanabe *et al*, 2010). Additionally, in the folded state, KLC is thought to contribute to the autoinhibition of kinesin-1 by pushing the KHC motor domains apart (Verhey *et al*, 1998; Cai *et al*, 2007). Binding to both KHC and KLC appears to be required to release the inhibition and to activate microtubule-dependent transport of kinesin-1 (Blasius *et al*, 2007; Verhey and Hammond, 2009). These findings, together with studies in KLC-deficient animals (Gindhart *et al*, 1998; Rahman *et al*, 1999), suggest that KLC may have a role in regulating kinesin-1 activity. However, several lines of evidence indicate that KLC is not essential for kinesin-1 activity and has a role in only some kinesin-1 transport events. Indeed, the tetrameric configuration is not obligatory and multiple lines of evidence suggest

*Corresponding author. Department of Anatomy and Neurobiology, Washington University School of Medicine, Campus Box 8108, 660 S. Euclid Ave, St Louis, MO 63110-1093, USA. Tel.: +1 314 362 3540; Fax: +1 314 362 3446; E-mail: cavalli@pcg.wustl.edu

Received: 5 January 2011; accepted: 21 June 2011; published online: 12 July 2011

that kinesin-1 exists and functions as a dimer of two heavy chains lacking the light chains: (i) KHC dimers can bind to membrane organelles in the absence of KLC (Skoufias *et al*, 1994); (ii) A small pool of KHC not associated with KLC has been found in various cultured cells and shown to possess motor properties of conventional tetrameric kinesin-1 (DeLuca *et al*, 2001; Gyoeva *et al*, 2004); (iii) In the retina, KLC does not fully colocalize with KHC and even appears to be absent from photoreceptors (Mavlyutov *et al*, 2002); and (iv) Cellular cargoes can be transported by direct interaction with KHC, without requiring KLC. For example, the adaptor protein syntabulin was shown to interact directly with KHC but not with KLC to promote the transport of syntaxin-containing vesicles (Su *et al*, 2004) and mitochondria (Cai *et al*, 2005). In *Drosophila*, the adaptor protein Milton attaches KHC to mitochondria in a KLC-independent manner (Cai *et al*, 2005; Glater *et al*, 2006) and mRNA transport is also KLC independent (Palacios and St Johnston, 2002; Loiseau *et al*, 2010).

In the absence of KLC, KHC activation relies on relieving the autoinhibition mediated by the KHC tail on the motor domain (Friedman and Vale, 1999; Coy *et al*, 1999a; Hackney and Stock, 2000, 2008; Cai *et al*, 2007; Cho *et al*, 2009; Wong *et al*, 2009). Recently, native cellular cargoes that are able to activate KHC directly have been identified. The Ran binding protein 2 (RanBP2) interacts with KHC (Cai *et al*, 2001; Cho *et al*, 2007) and activates the ATPase activity of KHC (Cho *et al*, 2009). The *Drosophila* Pat1 protein interacts with KHC and functions as a positive regulator of KHC motility for the transport of *oskar* mRNA and dynein in *Drosophila* oocytes (Loiseau *et al*, 2010).

To further understand KHC function within neurons, we examined the interaction of KHC with the adaptor protein Sunday Driver (syd). syd was identified in *Drosophila* in a genetic screen for axonal transport mutants and was shown to interact directly with KLC (Bowman *et al*, 2000). syd is a member of the JIP family of proteins, which interact with the c-Jun N-terminal kinase (JNK), and is thus also known as JIP3 (Kelkar *et al*, 2000) or JSAP1 (Ito *et al*, 1999). The *C. elegans* homologue of syd/JIP3 (unc-16) also integrates JNK signalling and kinesin-1-dependent transport (Byrd *et al*, 2001; Sakamoto *et al*, 2005). All known JIP family members interact with KLC (Bowman *et al*, 2000; Verhey *et al*, 2001; Kelkar *et al*, 2005; Nguyen *et al*, 2005; Sakamoto *et al*, 2005). The interaction between syd and KLC relies on syd's Leucine-Zipper (LZ) domain and on the KLC tetratricopeptide repeats (TPR domains) (Kelkar *et al*, 2005; Nguyen *et al*, 2005; Hammond *et al*, 2008). Given its interaction with kinesin, syd was proposed to mediate the axonal transport of at least one class of vesicles (Bowman *et al*, 2000). In *C. elegans*, syd/unc16 is involved in synaptic vesicle localization (Byrd *et al*, 2001; Sakamoto *et al*, 2005) and in synaptic membrane trafficking (Brown *et al*, 2009). Recently, we identified two different vesicle populations—endosomes and small anterogradely moving organelles—as syd cargoes in mouse axons (Abe *et al*, 2009). Here, we show that syd interacts directly with the tail domain of KHC in addition to and independently of its interaction with KLC. Using an *in vitro* motility assay, we show that syd activates KHC for microtubule-based transport and promotes efficient motility of KHC along microtubules, increasing both processive run length and velocity. Importantly, syd binding to KHC is functional in neurons, as syd mutants that bind KHC but not KLC are transported to axons and dendrites similarly to wild-type syd. syd's KHC-dependent transport does not rely on oligomerization with endogenous JIP family members. This work establishes syd as an adaptor for both kinesin-1 chains and as a positive regulator of kinesin-1 motility.

Results

syd interacts with KHC independently of KLC

To determine if syd's interaction with kinesin-1 is entirely dependent on KLC, we performed GST-pulldown assays combined with syd deletion analyses. N-terminal syd (N-syd), but not C-terminal syd (C-syd) was able to pull down both KLC and the neuron-specific kinesin heavy chain KIF5C, hereafter referred to as KHC (Figure 1A and B). VAMP3, an endosomal protein that does not bind to kinesin-1, is used as a negative control. Deletion of the LZ domain (N-sydΔLZ) resulted in loss of interaction with KLC1 and KLC2 (Figure 1C), consistent with previous observations (Verhey *et al*, 2001; Kelkar *et al*, 2005; Nguyen *et al*, 2005). However, N-sydΔLZ retained the ability to interact with KHC (Figure 1C). Deletion of the JNK binding domain or coiled-coil domains 2 and 3 did not prevent syd's interaction with either KLC or KHC (Figure 1C). Since KLC1 and KLC2 have almost identical TPR regions (Rahman *et al*, 1998) and interact with wild-type and mutant syd in a similar manner (Bowman *et al*, 2000), we focused our study on KLC1. To define the region interacting with KHC, we tested three N-syd fragments for their interaction with KHC and KLC. syd240–540, which contains the LZ domain, interacted with both KLC and KHC (Figure 1D). syd541–772, which lacks the LZ domain, did not interact with KHC or KLC (Figure 1D). However, syd3–239, which lacks the LZ domain, was not associated with KLC, as expected, but retained the ability to interact with KHC (Figure 1D), indicating that this syd fragment interacts with a KHC dimer lacking KLC.

To determine if a pool of KHC lacking the light chain exists in brain extract, we performed sucrose density centrifugation analysis. Similarly to what has been reported previously in cultured mammalian cells (DeLuca *et al*, 2001), we detected a population of KHC lacking the light chain in brain extracts (Figure 1E). The light chain was not degraded in these extracts and was detected in fractions of higher density along with a subset of KHC (Figure 1E). Quantification of KHC in the two distinct pools indicates that about 14% of KHC lacks the light chain. These results suggest that syd can associate with the pool of KHC that lacks KLC.

To determine the residues required for syd interaction with KHC, we generated a series of truncation mutants. This analysis revealed that aa50–80 was required to promote syd's interaction with KHC (Figure 2A and B). To determine if aa50–80 (hereafter referred to as *K*inesin-1 Heavy Chain *B*inding *D*omain, KBD) represents the minimal domain promoting syd–KHC interaction, we performed a deletion analysis. Deletion of the LZ domain abolished syd's interaction with KLC but not with KHC (Figures 1C and 2C). Deletion of the KBD did not prevent syd's interaction with tetrameric kinesin-1, consistent with the LZ domain interacting with KLC (Figure 2C). Since GFP–sydΔLZ binds to KHC dimer and GFP–sydΔKBD interacts with tetrameric kinesin-1 via KLC, deletion of both the KBD and LZ domains was required to

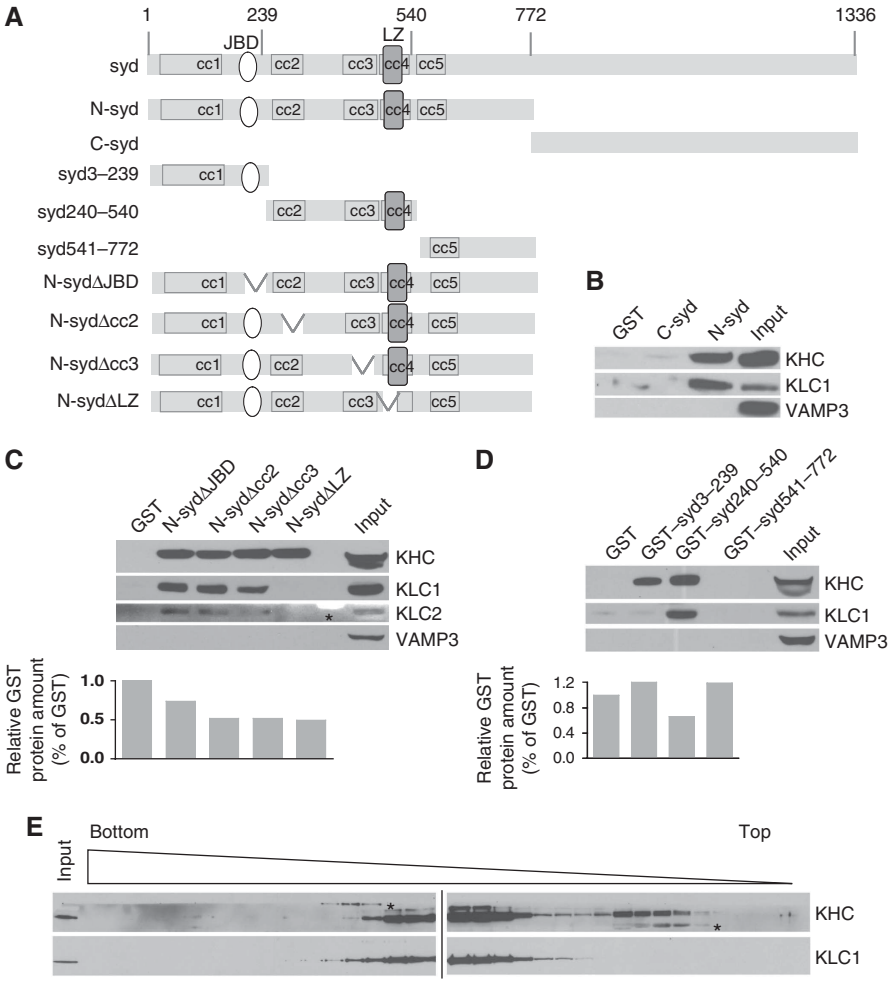

Figure 1 syd interacts with KHC independently of KLC. (**A**) Schematic illustration of full-length or truncated syd constructs used. Domains of known function located within the amino-terminal portion of syd (N-syd) are indicated. cc: coiled-coil domains; JBD: JNK binding domain; LZ: leucine-zipper domain (KLC binding domain). (**B**) Mouse brain lysate was used in pulldown experiments using recombinant GST, GST N-syd, or GST C-syd. Western blot analysis was performed with the indicated antibodies. VAMP3 was used as a negative control. Both KHC and KLC are pulled down with GST N-syd, but not with GST C-syd. (**C**) As in (**B**), but the indicated N-syd deletion mutants were used. N-syd lacking the KLC binding site (N-sydΔLZ) interacts with KHC but not KLC. The asterisk points to non-specific reaction with molecular marker loaded in this lane. (**D**) As in (**B**), but the indicated syd fragments were used. The syd fragment aa3–239, which does not contain the LZ domain is sufficient to bind KHC. Densitometry analysis of ponceau staining for (**C**) and (**D**) shows the relative amount of recombinant GST proteins used in each condition. Input for (**B**–**D**) is 10% of total starting material. (**E**) Active microtubule-bound kinesin-1 was released by ATP. The soluble kinesin-1 fraction was collected and separated by sucrose density gradient. The fractions were collected and analysed by western blot on two separate gels. The black separating line marks where separate gels have been spliced together. The asterisk points to non-specific crossreacting bands. A population of KHC is detected in lighter fractions at the top of the gradient, which does not contain KLC.

prevent syd's interaction with kinesin-1 (Figure 2C), indicating that the KBD is necessary for binding to KHC.

The C-terminal tail domain of KHC (aa807–956) mediates its interaction with several cargoes (reviewed in Hirokawa *et al*, 2009). To test whether syd binds the KHC tail domain, we conducted a GST-pulldown assay using a GST-tagged KHC tail (aa807–956). syd interacted with the GST–KHC tail, but not with GST alone (Figure 2D). To test whether syd directly binds to the KHC tail domain, we performed an *in vitro* binding assay using GST-tagged KHC tail (aa807–956), and His-tagged syd fragments. All three syd fragments containing the KBD interacted directly with the GST–KHC tail (Figure 2E). To determine whether the affinity between syd and KHC is similar to what has been previously measured between syd and KLC (Bowman *et al*, 2000), we performed a binding assay. Similarly to what has been reported (Bowman *et al*, 2000), we measured a Kd of 0.33 ± 0.08 μM between syd and KLC1-TPR (Figure 2F). The syd–KHC tail interaction displayed a lower affinity, with a Kd of 1.83 ± 0.43 μM (Figure 2G). Given the lower affinity of syd for KHC tail compared with KLC-TPR, syd may bind to a kinesin-1 tetramer containing both KHC and KLC, and syd binding to KHC may relieve or alter its autoinhibitory activity. However, kinesin-1 does not always exist as a tetramer, suggesting that syd can bind directly to a population of KHC that lacks KLC. Together, these results reveal an alternative and KLC-independent interaction between syd and kinesin-1.

syd's direct interaction with KHC is functional

To determine whether syd's interaction with KHC is functional, we analysed the dynamic properties of GFP-tagged syd by total internal reflection fluorescence microscopy (TIRF), as previously described (Blasius *et al*, 2007). COS cells

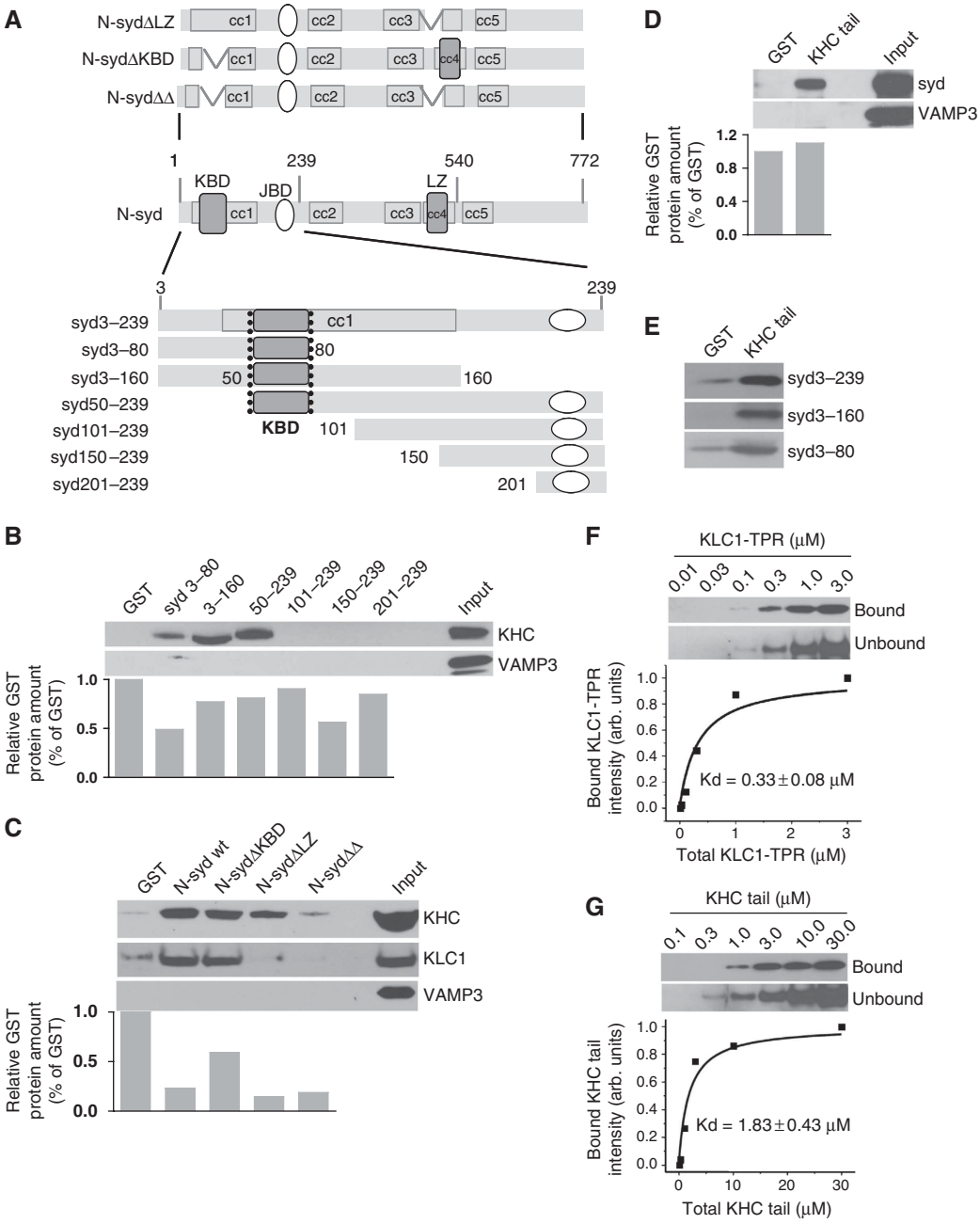

Figure 2 Mapping the syd domain necessary for KHC interaction. (**A**) Scheme of the constructs used in (**B**), (**C**), and **E**). (**B**) GST-pulldown analysis was conducted as described in Figure 1B. Residues 50–80 are required for syd interaction with KHC. VAMP3 is used as a negative control. (**C**) The indicated N-syd deletion mutants were used in a GST-pulldown assay and analysed by western blot with the indicated antibodies. Deletion of both LZ (KLC binding domain) and KBD (KHC binding domain) was required to prevent the syd–kinesin-1 interaction. (**D**) Recombinant GST–KHC tail (aa 807–956) was used in a GST-pulldown assay. The GST–KHC tail, but not GST, interacts with syd. Densitometry analysis of ponceau staining for (**B**–**D**) shows the relative amount of recombinant GST proteins used in each condition. Input is 10% of total starting material. (**E**) The indicated purified His-tagged syd fragments were incubated with purified GST or the GST–KHC tail. Direct binding of syd to the KHC tail domain was assessed using an anti-polyhistidine antibody. (**F**, **G**) Fixed amounts of recombinant GST N-syd (50 nM) were incubated with His–KLC1-TPR (**F**) or with His–KHC tail (**G**) at the indicated concentrations. The amount of bound His–KLC1-TPR or His–KHC tail was analysed by western blot with an anti-polyhistidine antibody and quantified using ImageJ. To estimate the dissociation constant, we plotted the band intensity for each concentration and used the first order binding equation: fraction of bound kinesin = [kinesin]/(Kd + [kinesin]), to fit the data generated.

were chosen for their low amounts of endogenous kinesin-1 (Cai *et al*, 2007) and were used to express the desired GFP–syd constructs or Flag–KHC. Cell lysates containing either Flag–KHC or GFP–syd were mixed before the motility assay, thereby ensuring identical amounts of KHC in each condition (Figure 3A). When lysate expressing GFP–syd wild-type (wt) was mixed with Flag–KHC lysate, motile events were observed (Figure 3B–D; see Supplementary Movie S1). However, when non-transfected cell extract was used in place of the Flag–KHC lysate, the absence of Flag–KHC dramatically reduced the number of motile events (Figure 3C and D; see Supplementary Movie S2), indicating that the low level of endogenous kinesin-1 in COS cells does not have a significant role under these conditions.

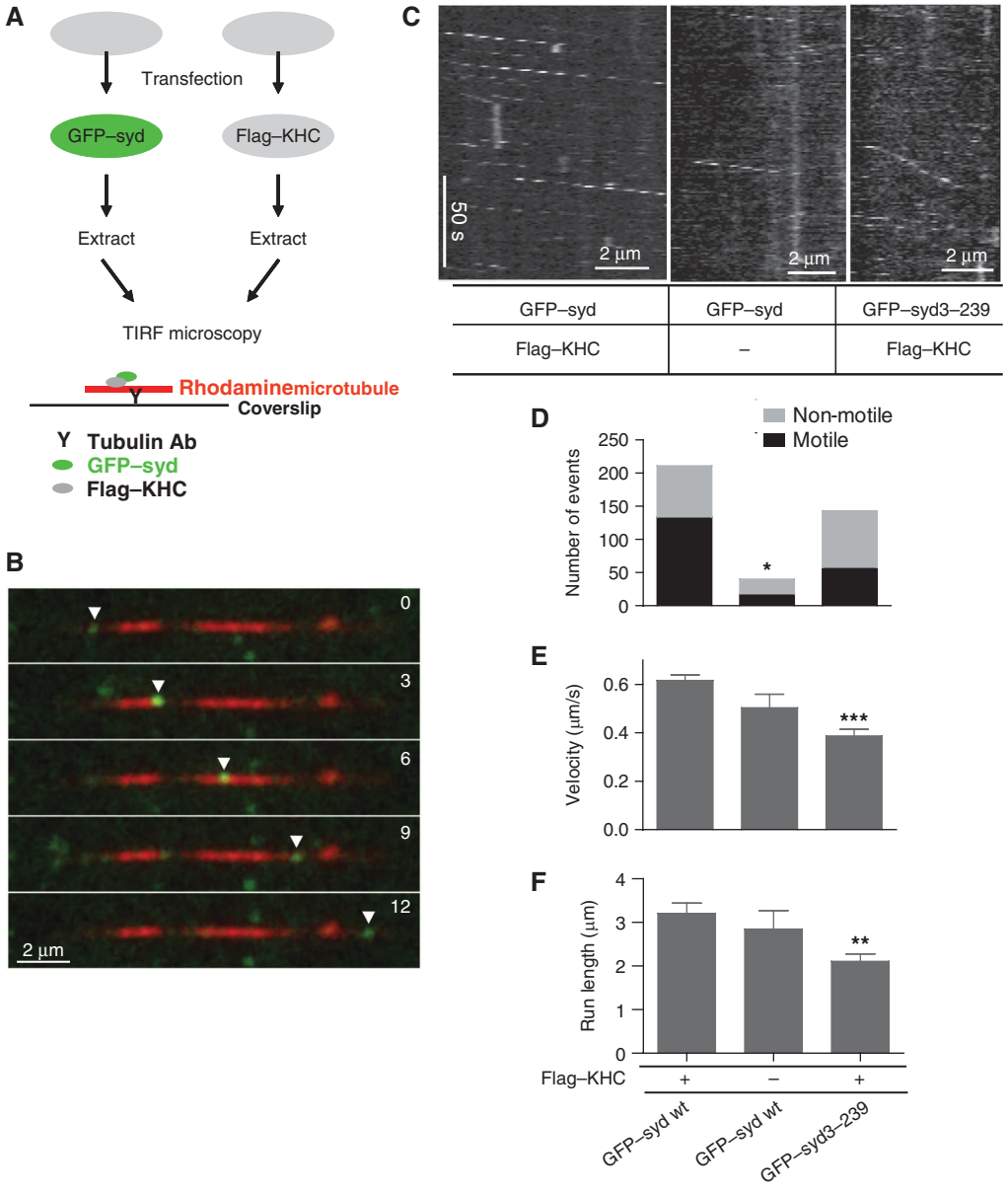

Figure 3 syd binding to KHC is functional. TIRF microscopy was used to visualize the KHC-dependent transport of GFP–syd along microtubules *in vitro*. (**A**) Scheme of the experimental procedures. COS-7 cells were transfected with the indicated GFP–syd constructs or Flag–KHC. Extracts were prepared and mixed just before TIRF assay. Non-transfected extract was used as a control for KHC-dependent movement. (**B**) Selected images from movie recorded with GFP–syd wt in the presence of KHC. The arrowheads mark the GFP–syd wt molecule movement on a microtubule over time (in seconds), bar: 2 µm. (**C**) Cell lysate expressing the indicated GFP–syd construct was mixed with lysate expressing Flag–KHC or non-transfected lysate as a control. Kymographs were generated from movies recorded for the indicated GFP–syd construct in the presence or absence of Flag–KHC. Vertical bar = 50 s, horizontal bar = 2 µm. (**D**) The proportion of motile versus non-motile events observed for each condition is shown. The difference in the probability for being motile or non-motile in each condition was analysed with χ^2 analysis. Data represent results of 3–4 independent experiments. One asterisk, $P<0.05$; compared with GFP–syd wt with KHC. (**E**) Calculated transport velocity for each condition. Velocity values represent mean ± s.e.m. of 15–101 motile events from 3 to 4 independent experiments. Compared with GFP–syd wt with KHC (Student's *t*-test), three asterisks, $P<0.001$. (**F**) Calculated run length for each condition. Run length values represent mean ± s.e.m. of 15–66 motile events from 3 to 4 independent experiments. Two asterisks $P<0.01$; compared with GFP–syd wt with KHC.

The movement of GFP–syd observed in these conditions is thus mainly mediated by its interaction with Flag–KHC. We measured a velocity of 0.62 ± 0.02 µm/s for GFP–syd wt (Figure 3E), which is similar to the velocity reported for kinesin-1 under comparable conditions (Blasius *et al*, 2007). The average run length we measured (3.21 ± 0.24 µm; Figure 3F) was greater than previously reported for kinesin-1 under comparable conditions (Blasius *et al*, 2007), but similar to purified recombinant kinesin-1 (Dixit *et al*, 2008).

We then tested whether GFP–syd3–239 binding to KHC was sufficient for motility. GFP–syd3–239 displayed motile events, albeit with reduced frequency compared with GFP–syd wt (Figure 3D; Supplementary Movie S3). Surprisingly, we observed that in addition to a reduced frequency of motile events, the velocity and run length decreased significantly for GFP–syd3–239, to 0.39 ± 0.03 µm/s and 2.11 ± 0.17 µm/run, respectively (Figure 3E and F). The reduced run length could be attributed to GFP–syd3–239 detaching from KHC sooner as

compared with GFP–syd wt. However, the reduced velocity observed for GFP–syd3–239 compared with GFP–syd wt suggests that other syd structural elements may participate in KHC regulation.

syd enhances KHC motility along microtubules

To directly determine whether syd regulates KHC motility, we next observed the movement of KHC–mCit in the presence or absence of Flag-tagged syd wt (Flag–syd wt; Figure 4A).

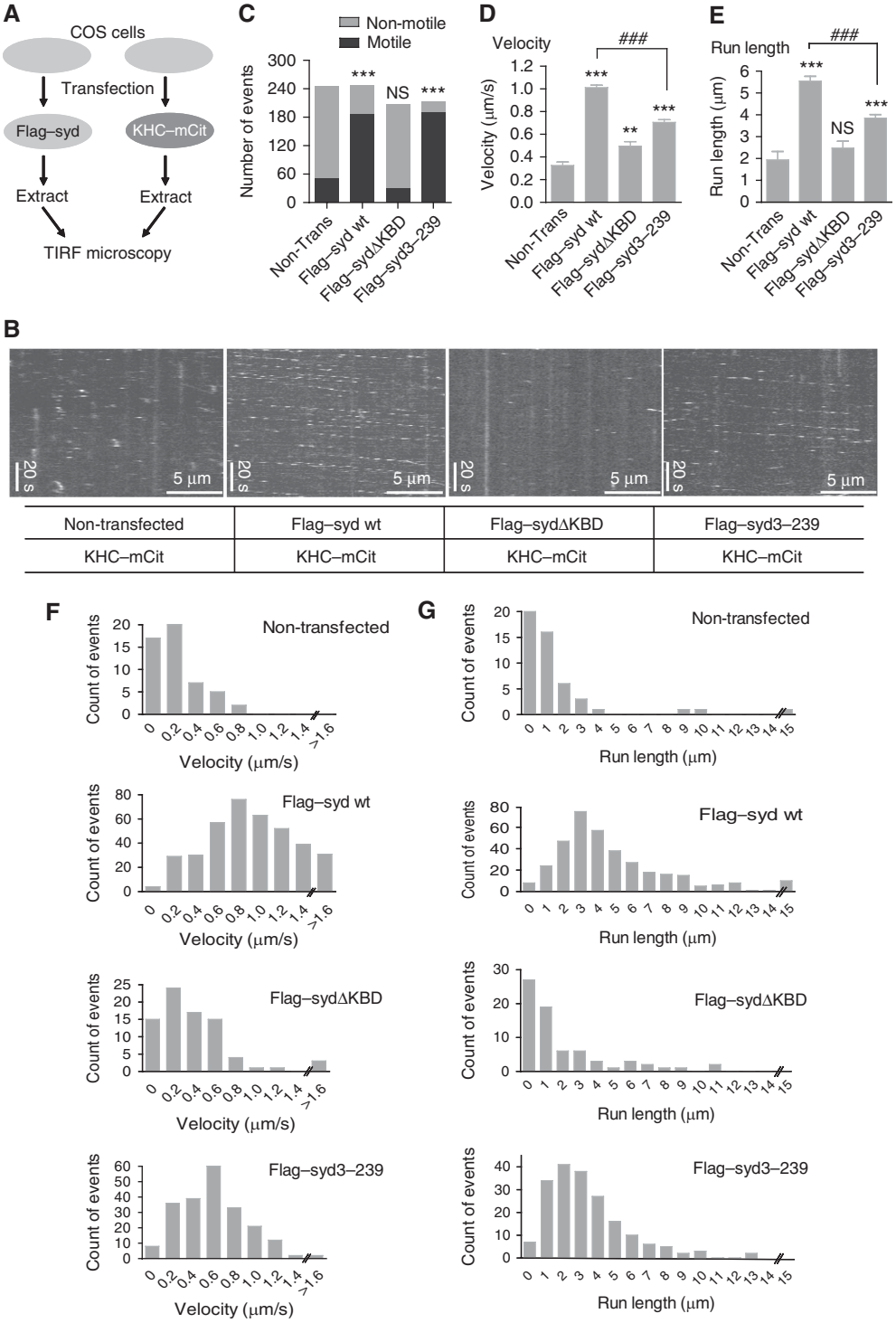

Figure 4 syd regulates kinesin-1 activity and motility. (**A**) Scheme of the experimental procedures. COS-7 cells were transfected with the indicated Flag–syd constructs or fluorescently tagged KHC at the C-terminus (KHC–mCit). (**B**) Kymographs were generated from movies recorded for KHC–mCit in the presence or absence of Flag–syd wt or in the presence of Flag–sydΔKBD or Flag–syd3–239. Vertical bar = 20 s, horizontal bar = 5 μm. (**C**) The proportion of motile versus non-motile events observed for each condition is shown. The difference in the probability for being motile or non-motile in each condition was analysed with χ^2 analysis. (**D**, **E**) Velocity (**D**) and run length (**E**) were calculated from the kymographs generated. Velocity and run length values represent mean ± s.e.m. of $n = 52$ for KHC–mCit alone, $n = 358$ for KHC–mCit with Flag–syd wt, $n = 76$ for KHC–mCit with Flag–sydΔKBD, $n = 191$ for KHC–mCit with Flag–syd3–239. Data were collected from 3 to 4 independent experiments. Asterisks (*): compared with non-transfected condition ($^{**}P < 0.01$, $^{***}P < 0.001$). Pound (#), compared with each other ($^{\#\#\#}P < 0.001$). (**F**, **G**) Raw distribution data are shown for velocity (**F**) and run length (**G**).

When mixed with non-transfected extracts, KHC–mCit displayed few motile events (Figure 4B and C), probably reflecting activation by endogenous adaptors in COS cells. We, however, collected sufficient motile events to analyse KHC–mCit motile properties. We measured a velocity of 0.33 ± 0.03 μm/s and a run length of 1.94 ± 0.39 μm/run (Figure 4D and E; see Figure 4F and G for the raw distribution; and Supplementary Movie S4), which is comparable to what has been reported previously for full-length kinesin-1 motility in similar assays (Sung *et al*, 2008; Loiseau *et al*, 2010). In the presence of Flag–syd wt, we observed a dramatic increase in the number of motile events (Figure 4B and C). Remarkably, we also observed a significant increase in velocity (1.01 ± 0.03 μm/s) and run length (5.54 ± 0.28 μm/run) (Figure 4D and E; see Figure 4F and G for the raw distribution data and Supplementary Movie S5). The velocity and run length of Flag–KHC in the presence of GFP–syd wt (Figure 3E and F) were found to be lower than that for KHC–mCit in the presence of Flag–syd wt (Figure 4D and E). This difference may result from the position of the tag, rendering Flag–KHC not as efficient as KHC–mCit. However, importantly, in both cases the presence of syd wt increased KHC motility. This increase in motility is likely due to syd binding to the KHC tail, since Flag–sydΔKBD only minimally affected KHC motility (Figure 4D and E; see Figure 4F and G for the raw distribution data; Supplementary Movie S6). This velocity is comparable to what has been measured for purified tail-less kinesin-1 (Hackney *et al*, 2003; Yildiz *et al*, 2008; Shastry and Hancock, 2010), indicating that syd's binding to the KHC tail is effective in relieving the inhibition of the motor domain by the KHC tail. However, the enhanced run length in the presence of syd is significantly greater than the run length reported for purified tail-less kinesin-1 (Dixit *et al*, 2008; Yildiz *et al*, 2008; Shastry and Hancock, 2010). Similarly to what we observed with GFP–syd3–239 motility (Figure 3E and F), we observed that Flag–syd 3–239 was able to activate KHC motility, but with reduced velocity and run length compared with Flag–syd wt (Figure 4D and E; see Figure 4F and G for the raw distribution data; Supplementary Movie S7). Together, these results indicate that binding of syd to KHC activates kinesin-1 for microtubule-dependent motion, enhancing both KHC velocity and run length, and that syd structural elements beyond the KHC binding site likely participate in KHC regulation. It is also possible that a small proportion of the observed motile events is mediated by a KHC–KLC tetramer. Indeed, we found that a small fraction of expressed KHC–mCit in COS cells can interact with endogenous KLC (Supplementary Figure S1). The relatively small increase in KHC velocity provided by Flag–sydΔKBD (Figure 4D) may thus represent an effect of Flag–sydΔKBD on a kinesin-1 tetramer via its interaction with KLC.

syd direct interaction with KHC promotes transport in neurons

To determine whether syd binding to KHC is sufficient for transport in neurons, we examined the localization of GFP–syd wt and mutants in cultured hippocampal neurons. Previous evidence suggests that syd localizes predominantly to axons during development and mostly to the cell bodies and dendrites in adult brain (Akechi *et al*, 2001; Setou *et al*, 2002). In agreement with these previous observations, we found that in cultured embryonic hippocampal neurons, endogenous syd is highly enriched at the tips of developing axons (Figure 5A). Similarly, expressed GFP–syd wt accumulated mostly at the tip of axons (Figure 5B, upper panel and 5E). GFP–sydΔLZ, which binds KHC, or GFP–sydΔKBD, which interacts with tetrameric kinesin-1 via KLC was transported equally to the axon tip (Figure 5B middle two panels and Figure 5E). GFP–syd wt, GFP–sydΔLZ, and GFP–sydΔKBD all displayed a similar low level distribution along dendrites (Figure 5C and E). In contrast, GFP–sydΔΔ failed to exit the cell body (Figure 5B and C bottom panel and Figure 5E) and was confined to the perinuclear region in proximity of the Golgi apparatus (Figure 5D). Lack of transport due to GFP–sydΔΔ misfolding is unlikely since GFP–sydΔΔ retains the ability to oligomerize with JIP family members in cells (Figure 6). Therefore, syd's interaction with KHC does not appear to specify axonal versus dendritic transport. Together, these results suggest that syd's interaction with KHC can mediate transport in neurons in the absence of the KLC binding site, as deletion of both KHC and KLC binding sites is required to prevent syd transport to axon tips.

syd/JIP family members are known to homo- or hetero-oligomerize (Yasuda *et al*, 1999; Kelkar *et al*, 2000, 2005; Kristensen *et al*, 2006; Hammond *et al*, 2008). To determine whether oligomerization with endogenous JIP family members bound to KLC mediates the transport of syd mutants, we first tested the ability of GFP-tagged syd mutants to oligomerize with Flag–syd wt. Flag–syd wt was co-transfected with GFP, GFP–syd3–239, GFP–syd wt, or GFP–sydΔΔ in N2A cells and immunoprecipitation was performed with anti-GFP antibodies. Flag–syd wt co-immunoprecipitated with GFP–syd3–239, GFP–sydΔΔ and GFP–syd wt but not with GFP alone, revealing that both GFP–syd3–239 and GFP–sydΔΔ can oligomerize, similarly to syd wt (Figure 6A). However, despite its ability to oligomerize with Flag–syd wt, GFP–sydΔΔ failed to exit the cell body (Figure 5C and D). Therefore, oligomerization of GFP–sydΔΔ with endogenous syd does not appear to be sufficient for its transport in neurons. We next examined the localization of mCherry–syd3–239 in cortical neurons prepared from mice lacking syd (Kelkar *et al*, 2003). Immunofluorescence of cultured cortical neurons (Figure 6B) and western blot analysis of brain lysates (Figure 6C) confirmed the lack of syd expression in *syd−/−* animals. We observed an enrichment of the syd mutants that bind KHC but not KLC, mCherry–syd3–239 and GFP–sydΔLZ, at the axonal tips of neurons lacking syd (Figure 6D–F). These results further exclude that oligomerization with endogenous syd mediates transport of syd mutants that bind KHC but not KLC.

syd can form hetero-oligomers with some JIP family members. In particular, syd can oligomerize with JIP2 and JIP1 (Kelkar *et al*, 2000; Hammond *et al*, 2008), but it does not oligomerize with JIP4 (Kelkar *et al*, 2005). While GFP–syd wt and GFP–sydΔΔ retained the ability to oligomerize with Flag–JIP2, GFP–syd3–239 failed to do so (Figure 6G). In contrast, all three constructs, GFP–syd wt, GFP–syd3–239 and GFP–sydΔΔ displayed the ability to oligomerize with myc–JIP1. Yet, despite its ability to oligomerize with myc–JIP1, GFP–sydΔΔ failed to exit the cell body (Figure 5C and D). This is in agreement with the results from Hammond *et al* (2008), showing that the formation of a JIP1/syd/KLC complex is necessary for efficient JIP1 or syd transport in

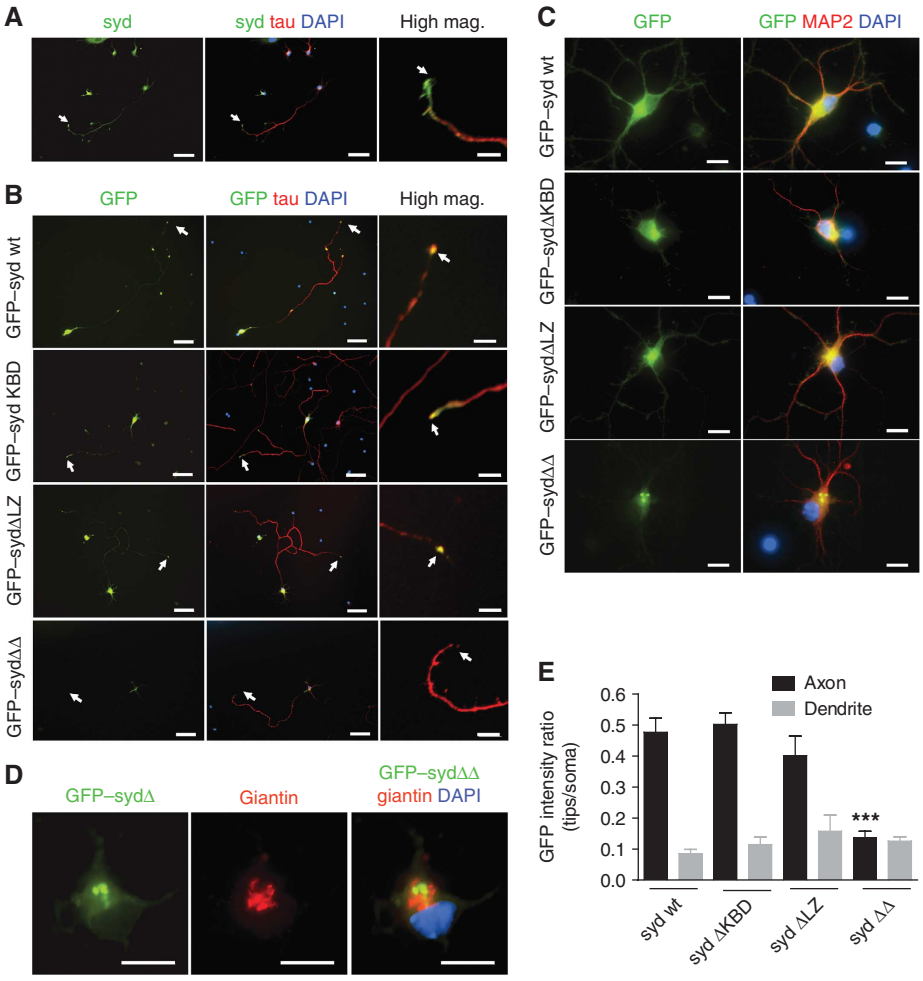

Figure 5 syd interaction with KHC is functional in neurons and mediates transport to both dendrites and axons. (**A**) E18 hippocampal neurons were stained for endogenous syd and the axonal marker tau. syd accumulates at the axonal tip. (**B**, **C**) Hippocampal neurons were transfected with the indicated GFP–syd constructs and stained with the axonal marker tau in (**B**) or the dendritic marker MAP2 in (**C**). Deletion of both LZ and KBD is required to prevent syd transport to axonal tips and proximal dendrites. (**D**) Deletion of both kinesin binding sites prevents exit from the cell body and leads to accumulation of syd in proximity of the Golgi apparatus stained with giantin antibody. (**E**) Quantification of syd accumulation in axon or dendritic tips. The ratio of GFP intensities between axon or dendrite tips and the somatic region was measured for each construct. Values are expressed as mean ± s.e.m. ($n = 12$–18), $^{***}P < 0.001$. Statistical difference was analysed for axon or dendrites categories between all conditions with the Student's *t*-test. (**A**–**C**) Bar = 50 μm, except that bar = 10 μm for high magnification (high mag.); arrows: axon tips; DAPI: nuclear marker.

neuronal cells. Thus, GFP–sydΔΔ and GFP–syd3–239 may be unable to be stably incorporated in a complex with JIP1 and KLC. Oligomerization with JIP1 may thus not fully account for the transport of syd lacking the KLC binding domain (GFP–syd3–239, Figure 6E). Although we cannot exclude that other yet unknown kinesin-1 binding proteins may be involved in syd transport in neurons, these results, together with our motility experiment, suggest that syd's interaction with KHC promotes transport in neurons.

Discussion

We report here that syd, a previously known KLC adaptor (Bowman *et al*, 2000), is also capable of interacting directly with KHC independently of KLC. Binding of syd to KHC not only activates kinesin-1 for microtubule-dependent transport, but also enhances KHC velocity and run length. Binding of syd to KHC is functional in neurons, since mutant syd that interacts with KHC only is targeted to axons and dendrites similarly to wt syd. Thus, syd–KHC interaction promotes transport but does not appear to determine transport specificity. Together, these data establish syd as a novel KHC binding partner capable of positively regulating kinesin-1 motility.

Regulation of kinesin-1 activity

Kinesin-1 is a processive motor, which takes multiple steps along microtubules before dissociating. How kinesin-1 activation for microtubule transport is controlled in live cells is not well understood, but recent studies couple kinesin-1 activation for microtubule transport with the binding of cellular partners (Blasius *et al*, 2007; Cho *et al*, 2009; Loiseau *et al*, 2010). A proposed regulatory mechanism for kinesin-1 activation is the transition from a 'folded' inactive state to an 'open' active state. In the inactive folded conformation, the KHC tail domain interacts with both the motor domain and the microtubules to prevent kinesin motion (Friedman and Vale, 1999; Hackney and Stock, 2000;

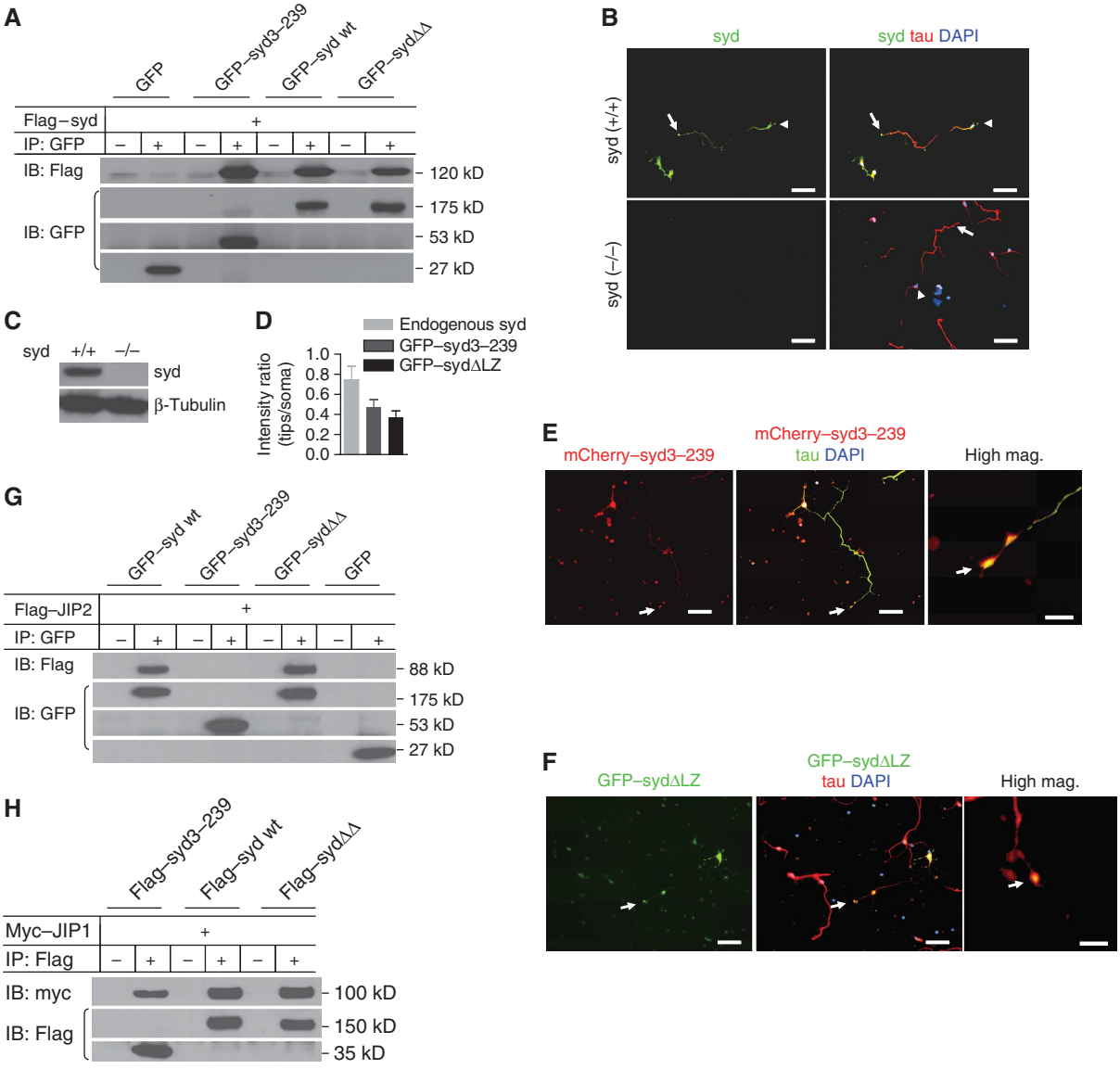

Figure 6 KHC-dependent syd transport does not depend on oligomerization with endogenous JIP family members. (**A**) Cell lysates were prepared from N2A cells transfected with Flag–syd together with GFP, GFP–syd3–239, GFP–syd wt, or GFP–sydΔΔ. Immunoprecipitation was performed with GFP antibodies or rabbit IgG as a negative control; western blots were probed with Flag and GFP antibodies. GFP–syd3–239 and GFP–sydΔΔ retain the ability to homo-oligomerize. (**B**) E18 cortical neurons from syd +/+ or *syd*−/− pups were stained with syd and tau, confirming the lack of expression in *syd*−/− neurons. (**C**) E18 brain lysates from wt (*syd*+/+) or *syd* knockout (*syd*−/−) were analysed by western blot. β-Tubulin is used as a loading control. (**D**) The ratio of fluorescence intensities between axon tips and the somatic region was measured for endogenous syd (stained with anti-syd antibody in *syd*+/+ neurons) and for the indicated GFP-constructs (GFP intensity in syd−/− neurons). (**E**, **F**) *syd*−/− cortical neurons were transfected with mCherry–syd3–239 (**E**) or GFP–sydΔLZ (**F**) and stained with the axon marker tau. Both constructs were transported to the axon tip. (**G**) Cell lysates were prepared from N2A cells transfected with Flag-tagged JIP2 together with GFP, GFP–syd3–239, GFP–syd wt, or GFP–sydΔΔ. Immunoprecipitation was performed with GFP antibodies or rabbit IgG as a negative control; western blots were probed with Flag and GFP antibodies. GFP–syd3–239 does not hetero-oligomerize with JIP2. (**H**) Cell lysates were prepared from N2A cells transfected with myc-tagged JIP1 together with Flag–syd wt, Flag–syd3–239, or Flag–sydΔΔ. Immunoprecipitation was performed with Flag antibodies or rabbit IgG as a negative control; western blots were probed with Flag and myc antibodies. All syd constructs oligomerize with JIP1. Arrows: axon tips; arrowheads: cell body. (**B**–**E**) Bar = 50 μm, except that bar = 10 μm for high magnification (high mag.).

Cai *et al*, 2007; Dietrich *et al*, 2008; Watanabe *et al*, 2010). Activation of kinesin-1 for transport requires a conformational change in which motor and tail domains are separated and the motor domains come closer together (Cai *et al*, 2007). Our *in vitro* motility results indicate that syd, but not sydΔKBD, which lacks the KHC binding domain, increased the number of motile events (Figure 4), suggesting that syd binding to the KHC tail domain efficiently relieves the inhibition by the KHC tail domain, activating or opening KHC to bind microtubules for long-range motility. These results place syd alongside Pat1 (Loiseau *et al*, 2010) and RanBP2 (Cho *et al*, 2009) as cellular regulators of kinesin-1 activity.

In the case of tetrameric kinesin-1, it has been proposed that binding of both KLC and KHC is required for motor activation (Blasius *et al*, 2007). It will be interesting to determine in future studies whether syd may fulfill activation of a KHC/KLC complex via its ability to interact with both KHC and KLC. Alternatively, similar to the JIP1–Fez1

complex (Blasius *et al*, 2007), syd may require additional interacting partners for the activation of tetrameric kinesin-1.

Regulation of kinesin-1 motility

Kinesin-1 stepping along microtubules is believed to involve concerted conformational change and diffusive movement of the tethered head to the next binding site. The precise mechanisms regulating the speed and the distance that kinesin-1 can achieve are fairly well understood for purified kinesin-1. Yet less is known about how kinesin-1 motility is regulated in a cellular environment. The observation that different kinesin-1 cargoes move at different rates in a cellular environment illustrates the complexity of *in vivo* motor regulation (Araki *et al*, 2007). The increase in KHC velocity and run length in the presence of full-length syd and syd3–239 suggests that syd binding to the KHC tail relieve the 'brake' provided by the tail binding to the microtubule (Dietrich *et al*, 2008; Seeger and Rice, 2010; Watanabe *et al*, 2010), thus allowing efficient forward movement. A recent study indicates that the *Drosophila* Pat1 protein interacts with KHC and functions as a positive regulator of KHC motility for the transport of *oskar* mRNA and dynein in *Drosophila* oocytes (Loiseau *et al*, 2010). In the absence of Pat1, both kinesin-1 velocity and run length are reduced (Loiseau *et al*, 2010). The Ran binding protein 2 (RanBP2) activates the ATPase activity of KHC (Cho *et al*, 2009), suggesting that RanBP2 may also regulate kinesin-1 velocity and processivity. These observations support the notion that adaptors contribute to regulate kinesin-1 motile properties, in addition to their roles in recruiting cargoes.

KLC-independent functions of KHC

Our results indicate that syd is capable of associating with both tetrameric and dimeric kinesin-1. This result is consistent with studies indicating that kinesin-1 exists and functions as a dimer of two heavy chains lacking the light chains, in addition to its conventional tetrameric conformation. KLC-independent transport has been reported for mitochondria (Cai *et al*, 2005; Glater *et al*, 2006), syntaxin-containing vesicles (Su *et al*, 2004), and RNA particles (Palacios and St Johnston, 2002; Kanai *et al*, 2004; Loiseau *et al*, 2010), in agreement with earlier studies reporting that KHC dimers can bind membrane organelles in the absence of KLC (Skoufias *et al*, 1994). Furthermore, a small pool of KHC not associated with KLC has been found in cultured HeLa cells and bovine brain (Hackney *et al*, 1991; DeLuca *et al*, 2001; Gyoeva *et al*, 2004) and we obtained similar results from mouse brain (Figure 1E). Degradation of KLC during kinesin-1 isolation can be excluded, since we detected KLC in our experiment (Figure 1E). Furthermore, significant molar excess of KHC over KLC has been reported in CV-1 cells (Gyoeva *et al*, 2004). It is thus conceivable that spatially and temporally, KHC and KLC do not always fully colocalize. Indeed, it has been shown that KLC is absent in photoreceptor cells and that throughout the retina, KLC does not fully colocalize with KHC (Mavlyutov *et al*, 2002), suggesting that at the cellular and subcellular levels KHC localization does not fully overlap with KLC. In addition, during brain development, KHC and KLC decline after the first week of postnatal life, but the decline in KLC appears to be more pronounced (Morfini *et al*, 2001). Therefore, it is possible that syd interacts with tetrameric kinesin-1 via KLC, while in cells or subcellular regions where KLC is absent syd instead interacts and regulates the activity of a kinesin-1 dimer. Our observation that syd interacts with KHC in addition to and independently from its known interaction with KLC is not inconsistent with the data published so far. In *C. elegans*, the localization of UNC-16 (syd) depends on both UNC-116 (KHC) and KLC (Sakamoto *et al*, 2005). Furthermore, syd transport to neurite tips in differentiated CAD cells is mostly, but not completely dependent on KLC (Verhey *et al*, 2001; Hammond *et al*, 2008). Similarly to syd, the FMRP was found to bind KLC (Dictenberg *et al*, 2008), and also KHC in a KLC-independent manner (Ling *et al*, 2004).

Syd role in axonal transport

Kinesin-1 drives different sets of cargoes to axons or dendrites, but how kinesin-1 distinguishes between axonal or dendritic cargoes for directional sorting remains poorly understood. Previous studies suggested that there was a dendritic preference for KHC cargoes and an axonal preference for KLC linkage (Setou *et al*, 2002; Hirokawa and Takemura, 2005). Our results showed that regardless of its mode of association with kinesin-1, syd is predominantly targeted to axon tips (Figure 5). It is thus more likely that the uploaded cargoes, and not the adaptor–motor complexes, determine the destination of kinesin-1 and its adaptor. We have recently shown that syd mediates the transport of at least two distinct types of vesicles in axons: endosomes and small anterogradely moving vesicles (Abe *et al*, 2009). It will be interesting to define in future studies the nature of the syd cargoes transported by KLC-dependent or KLC-independent interaction. Indeed, KLC isoforms have been proposed to mediate targeting of KHC to proper cargo (Stenoien and Brady, 1997; Khodjakov *et al*, 1998; Gyoeva *et al*, 2000; Wozniak and Allan, 2006), but KHC can also associate with membranous cargo in the absence of KLC (Skoufias *et al*, 1994).

The propensity of JIP family members to form homo or hetero-oligomers (Yasuda *et al*, 1999; Kelkar *et al*, 2000, 2005; Kristensen *et al*, 2006; Hammond *et al*, 2008; Koushika, 2008) suggests that syd may be transported via oligomerization. Indeed, Hammond *et al* (2008) reported that syd and JIP1 require each other for efficient transport of JIP1 or syd in non-neuronal cells. Such cooperative transport is due to an interaction between JIP1 and syd as well as distinct binding sites on the KLC-TPR domain. We found that despite its ability to oligomerize with myc–JIP1, GFP–sydΔΔ failed to exit the cell body (Figure 5C and D). Thus, GFP–sydΔΔ may be unable to be stably incorporated in a complex with JIP1 and KLC. Oligomerization with JIP1 may thus not fully account for the transport of the syd mutant GFP–syd3–239 lacking the KLC binding domain. Although we cannot exclude that other yet unknown kinesin-1 binding proteins may be involved in syd transport in neurons, our results suggest that syd's interaction with KHC may promote transport in neurons and that oligomerization may provide additional layers of regulation of syd-dependent transport.

In summary, we identified syd as an adaptor for kinesin-1 heavy chain and we determined that syd enhances KHC motility along microtubules. Future studies are needed to determine the precise mechanisms by which syd regulates kinesin-1 activation and processivity, and examine whether the distinct modes of syd interaction with kinesin-1 provide

specificity for cargo selection and delivery to particular subcelullar destinations.

Materials and methods

Antibodies and reagents

syd antibody was previously described (Bowman *et al*, 2000). The antibodies are as follows: anti-GFP (Invitrogen), anti-VAMP3 (Synaptic System), anti-kinesin heavy chain (KIF5C; Xia *et al*, 2003), anti-KLC1 (Santa Cruz), anti-KLC1–KLC2 (63–90) (gift from Dr Scott Brady), anti-His_6 (Qiagen), anti-Flag (Sigma), anti-β-tubulin (Sigma), anti-myc (Cell Signaling), anti-β-actin (Chemicon), anti-giantin (Abcam), anti-MAP2 (Chemicon), and anti-tau (Millipore). *syd* knockout mice were previously described (Kelkar *et al*, 2003). For wild-type animals, C57B6 mice were used.

Plasmid construction

KHC–mCit and myc–JIP1 were obtained from Dr Kristen Verhey and were previously described (Cai *et al*, 2007; Hammond *et al*, 2008). Full-length mouse syd cDNA was purchased from Open Biosystems (Huntsville, AL). Constructs for GST fusion proteins (N-terminal syd (aa 3–772), C-terminal syd (aa 773–1337), syd3–239, syd240–540, syd541–772, syd3–80, syd3–160, syd50–239, syd101–239, syd150–239, 201–239, syd429–459, syd50–82, KIF5C 807–956) were generated by inserting their coding sequences in-frame into the *Eco*RI and *Xho*I sites of the pGEX-4T-1 vector. Full-length clone of KHC (KIF5C) was isolated from a mouse cDNA library generated from adult mouse brain and inserted in-frame downstream of sequences encoding Flag in the pcDNA3 vector. To generate poly-histidine-tagged KLC1, KLC1-TPR (KLC1 177–413), syd3–80, syd3–160, syd3–239, KHC 807–956, the individual coding sequences were inserted into *Xho*I and *Eco*RI sites of pET-28a(+) vectors. GFP–syd and GFP–syd3–239 were obtained by ligating the coding sequences into *Xho*I and *Eco*RI sites of the pEGFP-C1 vector. mCherry–syd3–239 was generated by cloning syd3–239 into the mcherry-C1 vector. Flag–syd wt and mutants, and Flag–syd3–239 were generated by inserting their coding sequence in-frame downstream of sequences encoding a Flag tag in the pcDNA3 vector. A PCR-based overlap extension method (Pérez-Pinera, 2006) was used to construct the in-frame deletion mutants N-sydΔLZ (Δ429–459), N-sydΔKBD (Δ50–82), N-sydΔΔ (Δ50–82 and Δ429–459), N-sydΔJBD (Δ200–218), N-sydΔ266–315, N-sydΔ384–424, GFP–sydΔLZ, GFP–sydΔKBD, and GFP–sydΔΔ. All plasmids were sequenced and confirmed.

Recombinant protein purification

GST and His_6 fusion constructs were expressed in *E. coli* BL21 cells. For GST purification, following IPTG (0.5 mM) induction of protein expression, cells were harvested, resuspended in ice-cold PBS with 5.0 mM DTT and 1.0 mM AEBSF, and lysed with sonication. After addition of Triton X-100 (0.2%), the lysates were mixed at 4°C for 40 min, and the insoluble material was removed by centrifugation at 16 000 *g* for 30 min at 4°C. The clear lysates were then mixed with Glutathione Sepharose 4B beads (GE Healthcare) for 30 min at room temperature. The beads were washed with PBS three times, and GST fusion proteins were eluted with 20 mM reduced glutathione in Tris buffer (50 mM, pH 8.0). His_6-tagged proteins were purified using PrepEase His-tag resin (USB Corporation, Cleveland, OH). Briefly, cells were resuspended in LEW buffer (NaH_2PO_4 50 mM, NaCl 300 mM, AEBSF 1.0 mM, pH 8.0), sonicated and incubated with Triton X-100 (0.2%) for 40 min at 4°C. The lysates were clarified by centrifugation at 16 000 *g* for 30 min at 4°C and then mixed with resin at room temperature for 30 min. After three washings with LEW buffer, the bound His_6-tagged proteins are eluted with 250 mM imidazole in LEW buffer. The eluted recombinant proteins were dialysed in PBS or ultrafiltered for buffer exchange before their application.

GST pulldown and immunoprecipitation

GST pulldown. Mouse brains were homogenized in ice-cold lysis buffer (Tris–HCl 20 mM, NaCl, 200 mM, EDTA 1 mM, 0.5% Nonidet P-40, pH 8.0). The homogenate was centrifuged at 16 000 *g* for 20 min at 4°C, and the supernatant (1–2 mg) was incubated with Glutathione Sepharose 4B and equal molar amounts of purified GST fusion proteins or purified GST as negative control overnight at 4°C. The beads were collected by centrifugation at 500 *g* for 5 min at 4°C and washed three times with ice-cold PBS. Bound material was eluted by boiling beads in sample buffer for 5 min and analysed by western blot.

Immunoprecipitation. Dynabeads® Protein A Magnetic Beads (Invitrogen) were coated with anti-GFP antibody or rabbit IgG as a negative control, or with anti-myc with mouse IgG as a negative control. N2A cells were lysed in ice-cold lysis buffer 24 h after transfection and the lysate was incubated with coated magnetic beads for 2 h at 4°C on a rotating wheel. Beads were then washed three times with ice-cold PBS. The bound material was eluted by boiling beads in sample buffer for 5 min and analysed by western blot.

Protein binding assay. GST-tagged proteins were incubated with Glutathione Sepharose 4B beads for 30 min at room temperature, washed with PBS, and incubated with His_6-tagged proteins at 4°C on a rotating wheel for 90 min. Beads were washed three times with ice-cold PBS and bound material was eluted by boiling beads in sample buffer for 5 min and analysed by western blot. This assay was used to determine the dissociation constant between syd and KLC1-TPR and between syd and KHC tail, as previously described (Bowman *et al*, 2000). We used a fixed concentration of recombinant GST–syd N-terminal (50 nM) and various concentrations of the ligands His–KLC-TPR or His–KHC tail over a 3000-fold range. The relative amount of bound KLC1-TPR or KHC tail was analysed by western blot and quantified using ImageJ. The dissociation constants were measured by plotting the band intensity of bound kinesin for each concentration and using the first order binding equation: fraction of bound = [kinesin]/(Kd + [kinesin]) to fit the data.

Sucrose density centrifugation

Mouse brains were homogenized in PIPES buffer (50 mM PIPES, 1 mM EGTA, 1 mM $MgSO_4$, and protease inhibitors, pH 6.9). The homogenate was then centrifuged at 100 000 *g* for 30 min at 4°C to obtain a clear brain lysate. Glycerol (20%) and GTP (1 mM), taxol (20 μM) and AMP-PNP (2.5 mM) were added to brain lysates and incubated for 30 min at 37°C. The lysates were centrifuged at 100 000 *g* for 30 min at 22°C to pellet down microtubules and the associated kinesin motor. The resulting pellet was rinsed once with PIPES buffer with AMP-PNP (0.1 mM) and Taxol (20 μM). To release the motor from microtubules, the microtubule pellets were resuspended in ATP-containing buffer (100 mM PIPES, 1 mM EGTA, 1 mM $MgSO_4$, and ATP 20 mM, pH 6.9), and incubated for 1 h on ice. The re-suspension was then centrifuged as described above to collect the supernatant. The supernatant containing released motor proteins was loaded onto a sucrose gradient (5–50% in PIPES buffer), and centrifuged with a SW41 swinging bucket rotor for 14 h at 200 000 *g* at 4°C. Fractions were collected for western blot analysis with KHC and KLC antibodies.

In vitro motility assay

Twenty-four hours after transfection with the indicated constructs, COS cells were lysed with PIPES buffer with the addition of 1 mM EGTA and 0.1% Triton X-100. The supernatant was collected by centrifugation at 16 000 *g* for 15 min at 4°C. The *in vitro* motility assay was conducted as previously described (Dixit *et al*, 2008). Briefly, flow chambers were assembled from a glass slide and silanized coverslip attached using double-sided adhesive tape (chamber volume ~15 μl). In all, 250 nM microtubules were introduced in a flow chamber coated with 0.5% monoclonal anti-β tubulin antibody (Tub 2.1 clone, Sigma, St Louis, MO) and then blocked with 5% Pluronic F-127 (Sigma). COS cell extracts supplemented with 2 mM ATP, an oxygen scavenging system containing glucose oxidase, catalase, and glucose, and 10 mM DTT were subsequently flowed into the chamber. Single syd–GFP or KHC–mCit molecules were visualized at 25°C using TIRF microscopy outfitted on an inverted microscope (Olympus IX81). TIRF excitation was achieved using 488 and 532 nm diode-pumped solid-state lasers (Melles Griot) to visualize GFP and rhodamine, respectively. Low power laser (2 mW) allowed to track fluorescent particles over long distances. Images were captured with a back-thinned electron multiplier-CCD camera (ImagEM, Hamamatsu) at 1 s intervals. Non-transfected cell lysates were used for control experiments in parallel on the same day. The motion of GFP–syd or

KHC–mCit was analysed using kymographs generated with Slidebook (Intelligent Imaging Innovations). Vertical lines in kymographs were defined as non-motile events, while diagonal lines were defined as motile events. Only lines spanning more than two frames were counted as events. For non-motile events, only vertical lines with a fluorescence intensity similar to motile, diagonal lines were counted, to avoid inclusion of aggregates bound to microtubules.

Cell culture, transfection, and image analysis

N2A and COS-7 cells were grown in DMEM medium supplemented with 10% FBS, 1 mM sodium pyruvate, 2 mM L-glutamate, 0.1 mM non-essential amino acids and 1% Pen/Strep. Cells were grown on T25 flasks overnight before transfection using Lipofectamine 2000 (Invitrogen). Primary hippocampal and cortical cultures were prepared from mouse embryos at embryonic day 18 (E18). Hippocampi or cortices were treated with papain and DNase for 30 min, and triturated in neurobasal medium with 0.1% FBS. Dissociated neurons were cultured on coverslips coated with poly-D-lysine in Neurobasal medium containing 2% B27, 0.5 mM L-Glutamax and 1% Pen/Strep. About $5–6 \times 10^4$ neurons were plated per well in 24-well plates. Amaxa® Nucleofection® was used to transfect neurons before plating. After 5–6 days in culture, neurons were fixed in 4% paraformaldehyde in PBS with 4% sucrose for 10 min. Neurons were permeabilized and blocked with 10% goat serum, 0.1% Triton X-100 in PBS and incubated with the indicated primary antibodies and Alexa Fluor-conjugated secondary antibodies. Nuclei were stained by DAPI in the Prolong anti-fade mounting medium (Invitrogen). The images were acquired with fluorescence microscopy (Nikon, Eclipse TE 2000-E) and analysed with Nis-Element software.

Statistical analysis

Statistical analyses were performed using Student's *t*-test, except that χ^2 analysis was used to determine the statistical differences in motile frequency. For the motility experiments, the Kolmogorov–Smirnov test was used to test for normality of distribution. If the distribution was not normal, then statistical analysis was performed with the Kolmogorov–Smirnov test.

Supplementary data

Supplementary data are available at *The EMBO Journal* Online (http://www.embojournal.org).

Acknowledgements

We thank Drs Karen O'Malley and Vitaly Klyachko, and the Cavalli laboratory members for critical reading of the manuscript. We are grateful to Tammy Kershner for technical assistance. We thank Dr Roger Davis for providing the *syd* KO mice and Dr Kristen Verhey for providing the KHC–mCit and myc–JIP1 constructs. This work was supported in part by National Institutes of Health Grant RO1NS060709 from NINDS and the Edward Mallinckrodt Jr Foundation (to VC). This work was also supported by a Craig Neilsen Foundation postdoctoral fellowship (to FS).

Author contributions: FS and VC designed the experiments. FS performed all biochemical and cellular experiments and data analysis. FS and CZ performed and analysed the *in vitro* motility assay. RD guided and supervised the *in vitro* motility experiments. FS, RD, and VC wrote the manuscript.

Conflict of interest

The authors declare that they have no conflict of interest.

References

Abe N, Almenar-Queralt A, Lillo C, Shen Z, Lozach J, Briggs SP, Williams DS, Goldstein LS, Cavalli V (2009) Sunday driver interacts with two distinct classes of axonal organelles. *J Biol Chem* **284:** 34628–34639

Akechi M, Ito M, Uemura K, Takamatsu N, Yamashita S, Uchiyama K, Yoshioka K, Shiba T (2001) Expression of JNK cascade scaffold protein JSAP1 in the mouse nervous system. *Neurosci Res* **39:** 391–400

Aoyama T, Hata S, Nakao T, Tanigawa Y, Oka C, Kawaichi M (2009) Cayman ataxia protein caytaxin is transported by kinesin along neurites through binding to kinesin light chains. *J Cell Sci* **122:** 4177–4185

Araki Y, Kawano T, Taru H, Saito Y, Wada S, Miyamoto K, Kobayashi H, Ishikawa HO, Ohsugi Y, Yamamoto T, Matsuno K, Kinjo M, Suzuki T (2007) The novel cargo Alcadein induces vesicle association of kinesin-1 motor components and activates axonal transport. *EMBO J* **26:** 1475–1486

Blasius TL, Cai D, Jih GT, Toret CP, Verhey KJ (2007) Two binding partners cooperate to activate the molecular motor Kinesin-1. *J Cell Biol* **176:** 11–17

Bowman AB, Kamal A, Ritchings BW, Philp AV, McGrail M, Gindhart JG, Goldstein LS (2000) Kinesin-dependent axonal transport is mediated by the sunday driver (SYD) protein. *Cell* **103:** 583–594

Bracale A, Cesca F, Neubrand VE, Newsome TP, Way M, Schiavo G (2007) Kidins220/ARMS is transported by a kinesin-1-based mechanism likely to be involved in neuronal differentiation. *Mol Biol Cell* **18:** 142–152

Brown HM, Van Epps HA, Goncharov A, Grant BD, Jin Y (2009) The JIP3 scaffold protein UNC-16 regulates RAB-5 dependent membrane trafficking at C. elegans synapses. *Dev Neurobiol* **69:** 174–190

Byrd DT, Kawasaki M, Walcoff M, Hisamoto N, Matsumoto K, Jin Y (2001) UNC-16, a JNK-signaling scaffold protein, regulates vesicle transport in C. elegans. *Neuron* **32:** 787–800

Cai D, Hoppe AD, Swanson JA, Verhey KJ (2007) Kinesin-1 structural organization and conformational changes revealed by FRET stoichiometry in live cells. *J Cell Biol* **176:** 51–63

Cai Q, Gerwin C, Sheng ZH (2005) Syntabulin-mediated anterograde transport of mitochondria along neuronal processes. *J Cell Biol* **170:** 959–969

Cai Y, Singh BB, Aslanukov A, Zhao H, Ferreira PA (2001) The docking of kinesins, KIF5B and KIF5C, to Ran-binding protein 2 (RanBP2) is mediated via a novel RanBP2 domain. *J Biol Chem* **276:** 41594–41602

Cho KI, Cai Y, Yi H, Yeh A, Aslanukov A, Ferreira PA (2007) Association of the kinesin-binding domain of RanBP2 to KIF5B and KIF5C determines mitochondria localization and function. *Traffic* **8:** 1722–1735

Cho KI, Yi H, Desai R, Hand AR, Haas AL, Ferreira PA (2009) RANBP2 is an allosteric activator of the conventional kinesin-1 motor protein, KIF5B, in a minimal cell-free system. *EMBO Rep* **10:** 480–486

Coy DL, Hancock WO, Wagenbach M, Howard J (1999a) Kinesin's tail domain is an inhibitory regulator of the motor domain. *Nat Cell Biol* **1:** 288–292

DeLuca JG, Newton CN, Himes RH, Jordan MA, Wilson L (2001) Purification and characterization of native conventional kinesin, HSET, and CENP-E from mitotic hela cells. *J Biol Chem* **276:** 28014–28021

Dictenberg JB, Swanger SA, Antar LN, Singer RH, Bassell GJ (2008) A direct role for FMRP in activity-dependent dendritic mRNA transport links filopodial-spine morphogenesis to fragile X syndrome. *Dev Cell* **14:** 926–939

Diefenbach RJ, Diefenbach E, Douglas MW, Cunningham AL (2002) The heavy chain of conventional kinesin interacts with the SNARE proteins SNAP25 and SNAP23. *Biochemistry* **41:** 14906–14915

Dietrich KA, Sindelar CV, Brewer PD, Downing KH, Cremo CR, Rice SE (2008) The kinesin-1 motor protein is regulated by a direct interaction of its head and tail. *Proc Natl Acad Sci USA* **105:** 8938–8943

Dixit R, Ross JL, Goldman YE, Holzbaur EL (2008) Differential regulation of dynein and kinesin motor proteins by tau. *Science* **319:** 1086–1089

Friedman DS, Vale RD (1999) Single-molecule analysis of kinesin motility reveals regulation by the cargo-binding tail domain. *Nat Cell Biol* **1:** 293–297

Gindhart JG, Chen J, Faulkner M, Gandhi R, Doerner K, Wisniewski T, Nandlestadt A (2003) The kinesin-associated protein UNC-76 is

required for axonal transport in the Drosophila nervous system. *Mol Biol Cell* **14:** 3356–3365

Gindhart Jr JG, Desai CJ, Beushausen S, Zinn K, Goldstein LS (1998) Kinesin light chains are essential for axonal transport in Drosophila. *J Cell Biol* **141:** 443–454

Glater EE, Megeath LJ, Stowers RS, Schwarz TL (2006) Axonal transport of mitochondria requires milton to recruit kinesin heavy chain and is light chain independent. *J Cell Biol* **173:** 545–557

Goldstein AY, Wang X, Schwarz TL (2008) Axonal transport and the delivery of pre-synaptic components. *Curr Opin Neurobiol* **18:** 495–503

Grigoriev I, Splinter D, Keijzer N, Wulf PS, Demmers J, Ohtsuka T, Modesti M, Maly IV, Grosveld F, Hoogenraad CC, Akhmanova A (2007) Rab6 regulates transport and targeting of exocytotic carriers. *Dev Cell* **13:** 305–314

Guzik BW, Goldstein LS (2004) Microtubule-dependent transport in neurons: steps towards an understanding of regulation, function and dysfunction. *Curr Opin Cell Biol* **16:** 443–450

Gyoeva FK, Bybikova EM, Minin AA (2000) An isoform of kinesin light chain specific for the Golgi complex. *J Cell Sci* **113** (Pt 11)**:** 2047–2054

Gyoeva FK, Sarkisov DV, Khodjakov AL, Minin AA (2004) The tetrameric molecule of conventional kinesin contains identical light chains. *Biochemistry* **43:** 13525–13531

Hackney DD, Levitt JD, Wagner DD (1991) Characterization of alpha 2 beta 2 and alpha 2 forms of kinesin. *Biochem Biophys Res Commun* **174:** 810–815

Hackney DD, Stock MF (2000) Kinesin's IAK tail domain inhibits initial microtubule-stimulated ADP release. *Nat Cell Biol* **2:** 257–260

Hackney DD, Stock MF (2008) Kinesin tail domains and Mg2 + directly inhibit release of ADP from head domains in the absence of microtubules. *Biochemistry* **47:** 7770–7778

Hackney DD, Stock MF, Moore J, Patterson RA (2003) Modulation of kinesin half-site ADP release and kinetic processivity by a spacer between the head groups. *Biochemistry* **42:** 12011–12018

Hammond JW, Griffin K, Jih GT, Stuckey J, Verhey KJ (2008) Co-operative versus independent transport of different cargoes by Kinesin-1. *Traffic* **9:** 725–741

Hirokawa N, Noda Y, Tanaka Y, Niwa S (2009) Kinesin superfamily motor proteins and intracellular transport. *Nat Rev Mol Cell Biol* **10:** 682–696

Hirokawa N, Takemura R (2005) Molecular motors and mechanisms of directional transport in neurons. *Nat Rev Neurosci* **6:** 201–214

Ito M, Yoshioka K, Akechi M, Yamashita S, Takamatsu N, Sugiyama K, Hibi M, Nakabeppu Y, Shiba T, Yamamoto KI (1999) JSAP1, a novel jun N-terminal protein kinase (JNK)-binding protein that functions as a Scaffold factor in the JNK signaling pathway. *Mol Cell Biol* **19:** 7539–7548

Kamal A, Stokin GB, Yang Z, Xia CH, Goldstein LS (2000) Axonal transport of amyloid precursor protein is mediated by direct binding to the kinesin light chain subunit of kinesin-I. *Neuron* **28:** 449–459

Kanai Y, Dohmae N, Hirokawa N (2004) Kinesin transports RNA: isolation and characterization of an RNA-transporting granule. *Neuron* **43:** 513–525

Kelkar N, Delmotte MH, Weston CR, Barrett T, Sheppard BJ, Flavell RA, Davis RJ (2003) Morphogenesis of the telencephalic commissure requires scaffold protein JNK-interacting protein 3 (JIP3). *Proc Natl Acad Sci USA* **100:** 9843–9848

Kelkar N, Gupta S, Dickens M, Davis RJ (2000) Interaction of a mitogen-activated protein kinase signaling module with the neuronal protein JIP3. *Mol Cell Biol* **20:** 1030–1043

Kelkar N, Standen CL, Davis RJ (2005) Role of the JIP4 scaffold protein in the regulation of mitogen-activated protein kinase signaling pathways. *Mol Cell Biol* **25:** 2733–2743

Khodjakov A, Lizunova EM, Minin AA, Koonce MP, Gyoeva FK (1998) A specific light chain of kinesin associates with mitochondria in cultured cells. *Mol Biol Cell* **9:** 333–343

Kimura T, Watanabe H, Iwamatsu A, Kaibuchi K (2005) Tubulin and CRMP-2 complex is transported via Kinesin-1. *J Neurochem* **93:** 1371–1382

Konecna A, Frischknecht R, Kinter J, Ludwig A, Steuble M, Meskenaite V, Indermuhle M, Engel M, Cen C, Mateos JM, Streit P, Sonderegger P (2006) Calsyntenin-1 docks vesicular cargo to kinesin-1. *Mol Biol Cell* **17:** 3651–3663

Koushika SP (2008) 'JIP'ing along the axon: the complex roles of JIPs in axonal transport. *Bioessays* **30:** 10–14

Kristensen O, Guenat S, Dar I, Allaman-Pillet N, Abderrahmani A, Ferdaoussi M, Roduit R, Maurer F, Beckmann JS, Kastrup JS, Gajhede M, Bonny C (2006) A unique set of SH3-SH3 interactions controls IB1 homodimerization. *EMBO J* **25:** 785–797

Ling SC, Fahrner PS, Greenough WT, Gelfand VI (2004) Transport of Drosophila fragile X mental retardation protein-containing ribonucleoprotein granules by kinesin-1 and cytoplasmic dynein. *Proc Natl Acad Sci USA* **101:** 17428–17433

Loiseau P, Davies T, Williams LS, Mishima M, Palacios IM (2010) Drosophila PAT1 is required for Kinesin-1 to transport cargo and to maximize its motility. *Development* **137:** 2763–2772

Mavlyutov TA, Cai Y, Ferreira PA (2002) Identification of RanBP2- and kinesin-mediated transport pathways with restricted neuronal and subcellular localization. *Traffic* **3:** 630–640

Morfini G, Szebenyi G, Richards B, Brady ST (2001) Regulation of kinesin: implications for neuronal development. *Dev Neurosci* **23:** 364–376

Nguyen Q, Lee CM, Le A, Reddy EP (2005) JLP associates with kinesin light chain 1 through a novel leucine zipper-like domain. *J Biol Chem* **280:** 30185–30191

Palacios IM, St Johnston D (2002) Kinesin light chain-independent function of the Kinesin heavy chain in cytoplasmic streaming and posterior localisation in the Drosophila oocyte. *Development* **129:** 5473–5485

Pérez-Pinera P (2006) Deletion of DNA sequences of using a polymerase chain reaction based. *Electronic J Biotechnol* **9:** 604–609

Rahman A, Friedman DS, Goldstein LS (1998) Two kinesin light chain genes in mice. Identification and characterization of the encoded proteins. *J Biol Chem* **273:** 15395–15403

Rahman A, Kamal A, Roberts EA, Goldstein LS (1999) Defective kinesin heavy chain behavior in mouse kinesin light chain mutants. *J Cell Biol* **146:** 1277–1288

Roux KJ, Crisp ML, Liu Q, Kim D, Kozlov S, Stewart CL, Burke B (2009) Nesprin 4 is an outer nuclear membrane protein that can induce kinesin-mediated cell polarization. *Proc Natl Acad Sci USA* **106:** 2194–2199

Sakamoto R, Byrd DT, Brown HM, Hisamoto N, Matsumoto K, Jin Y (2005) The Caenorhabditis elegans UNC-14 RUN domain protein binds to the kinesin-1 and UNC-16 complex and regulates synaptic vesicle localization. *Mol Biol Cell* **16:** 483–496

Seeger MA, Rice SE (2010) Microtubule-associated protein-like binding of the kinesin-1 tail to microtubules. *J Biol Chem* **285:** 8155–8162

Setou M, Seog DH, Tanaka Y, Kanai Y, Takei Y, Kawagishi M, Hirokawa N (2002) Glutamate-receptor-interacting protein GRIP1 directly steers kinesin to dendrites. *Nature* **417:** 83–87

Shastry S, Hancock WO (2010) Neck linker length determines the degree of processivity in kinesin-1 and kinesin-2 motors. *Curr Biol* **20:** 939–943

Skoufias DA, Cole DG, Wedaman KP, Scholey JM (1994) The carboxyl-terminal domain of kinesin heavy chain is important for membrane binding. *J Biol Chem* **269:** 1477–1485

Stenoien DL, Brady ST (1997) Immunochemical analysis of kinesin light chain function. *Mol Biol Cell* **8:** 675–689

Su Q, Cai Q, Gerwin C, Smith CL, Sheng ZH (2004) Syntabulin is a microtubule-associated protein implicated in syntaxin transport in neurons. *Nat Cell Biol* **6:** 941–953

Sung HH, Telley IA, Papadaki P, Ephrussi A, Surrey T, Rorth P (2008) Drosophila ensconsin promotes productive recruitment of Kinesin-1 to microtubules. *Dev Cell* **15:** 866–876

Taya S, Shinoda T, Tsuboi D, Asaki J, Nagai K, Hikita T, Kuroda S, Kuroda K, Shimizu M, Hirotsune S, Iwamatsu A, Kaibuchi K (2007) DISC1 regulates the transport of the NUDEL/LIS1/14-3-3epsilon complex through kinesin-1. *J Neurosci* **27:** 15–26

Terada S, Kinjo M, Aihara M, Takei Y, Hirokawa N (2010) Kinesin-1/Hsc70-dependent mechanism of slow axonal transport and its relation to fast axonal transport. *EMBO J* **29:** 843–854

Verhey KJ, Hammond JW (2009) Traffic control: regulation of kinesin motors. *Nat Rev Mol Cell Biol* **10:** 765–777

Verhey KJ, Lizotte DL, Abramson T, Barenboim L, Schnapp BJ, Rapoport TA (1998) Light chain-dependent regulation of Kinesin's interaction with microtubules. *J Cell Biol* **143:** 1053–1066

Verhey KJ, Meyer D, Deehan R, Blenis J, Schnapp BJ, Rapoport TA, Margolis B (2001) Cargo of kinesin identified as JIP scaffolding proteins and associated signaling molecules. *J Cell Biol* **152:** 959–970

Watanabe TM, Yanagida T, Iwane AH (2010) Single molecular observation of self-regulated Kinesin motility. *Biochemistry* **49:** 4654–4661

Wong YL, Dietrich KA, Naber N, Cooke R, Rice SE (2009) The Kinesin-1 tail conformationally restricts the nucleotide pocket. *Biophys J* **96:** 2799–2807

Wozniak MJ, Allan VJ (2006) Cargo selection by specific kinesin light chain 1 isoforms. *EMBO J* **25:** 5457–5468

Xia CH, Roberts EA, Her LS, Liu X, Williams DS, Cleveland DW, Goldstein LS (2003) Abnormal neurofilament transport caused by targeted disruption of neuronal kinesin heavy chain KIF5A. *J Cell Biol* **161:** 55–66

Yamada M, Toba S, Takitoh T, Yoshida Y, Mori D, Nakamura T, Iwane AH, Yanagida T, Imai H, Yu-Lee LY, Schroer T, Wynshaw-Boris A, Hirotsune S (2010) mNUDC is required for plus-end-directed transport of cytoplasmic dynein and dynactins by kinesin-1. *EMBO J* **29:** 517–531

Yasuda J, Whitmarsh AJ, Cavanagh J, Sharma M, Davis RJ (1999) The JIP group of mitogen-activated protein kinase scaffold proteins. *Mol Cell Biol* **19:** 7245–7254

Yildiz A, Tomishige M, Gennerich A, Vale RD (2008) Intramolecular strain coordinates kinesin stepping behavior along microtubules. *Cell* **134:** 1030–1041